Flinders UNIVERSITY

Accepted Manuscript

Polydopamine as sizing on carbon fiber surfaces for enhancement of epoxy laminated composites

Wei Han, Hong-Ping Zhang, Javad Tavakoli, Jonathan Campbell, Youhong Tang

PII: S1359-835X(18)30043-5
DOI: https://doi.org/10.1016/j.compositesa.2018.02.003
Reference: JCOMA 4917

To appear in: *Composites: Part A*

Received Date: 15 November 2017
Revised Date: 17 January 2018
Accepted Date: 2 February 2018

Please cite this article as: Han, W., Zhang, H-P., Tavakoli, J., Campbell, J., Tang, Y., Polydopamine as sizing on carbon fiber surfaces for enhancement of epoxy laminated composites, *Composites: Part A* (2018), doi: https://doi.org/10.1016/j.compositesa.2018.02.003

Polydopamine as sizing on carbon fiber surfaces for enhancement of epoxy laminated composites

Wei Han [1], Hong-Ping Zhang [1, 2], Javad Tavakoli [1], Jonathan Campbell [1], Youhong Tang [1, *]

[1] College of Science and Engineering, Flinders University, South Australia 5042, Australia

[2] School of Materials Science and Engineering, Southwest University of Science and Technology, Mianyang, Sichuan 621010, China

[*] Corresponding author. Tel.: 61-8-82012138, email: youhong.tang@flinders.edu.au (Y Tang)

Abstract

Carbon fiber reinforced polymer (CFRP) laminate normally has plastic dominant crack propagation behavior, inducing potential insecurity in the safety and reliability of structures in practical applications. In this study, we report a simple process to increase the stability of crack growth by using polydopamine (PDA) as sizing on the surface of carbon fiber (CF) fabric. The crack propagation behavior changes from a saw-tooth-shaped curve in neat CFRP laminate to a relatively smooth trending curve in PDA coated CFRP laminate with increased Mode I interlaminar fracture toughness. Enhanced impact strength and interlaminar shear strength of PDA coated CFRP laminates is also observed. A single fiber pull-out experiment and morphological study reveal that, with PDA coating on CF fabrics, cracks tend to fracture through the epoxy matrix rather than between fiber and matrix interfaces. The use of PDA as sizing on the CF contributes to improving the load transfer between the CF and the polymer matrix by enhancing the interfaces between the epoxy and the CF, increasing the friction of the fractured interface, reducing unstable crack growth, and thereby enhancing interfacial fracture toughness and impact performance.

Keywords: A. Carbon fibres; B. Delamination, Fibre/matrix bond, Surface properties.

1. Introduction

Carbon fiber reinforced polymer (CFRP) is an extremely strong and light material that is now widely used in high value-added commodities wherever high strength-to-weight ratio and rigidity are required, such as in aerospace, automotive, civil engineering, and sports goods applications. For example, the Airbus A350 XWB was built of 52% CFRP including wing spars and fuselage components. One of the major problems that limits the stability and application range of CFRP is that the binding polymer is often a thermoset resin such as epoxy, but epoxy is a brittle material, so that the mechanical properties of the epoxy resin, especially the strength and toughness, still need to be further enhanced [1-6]. Engineers face unique challenges in failure detection of CFRP because failure occurs catastrophically due to the brittle fracture mechanics. Meanwhile, CFRP tends to be strengthened in the fiber horizontal direction when load-bearing occurs in that direction, but is weak in the vertical direction so that little load could be placed in that direction. Study of the mechanisms of the fracture toughness of CFRP is mainly governed by the subsequent debonding appearance, i.e., debonding between the carbon fiber (CF) and polymer matrix, fiber pull-out, and delamination between the CFRP sheets. Therefore, many researchers have studied how to toughen the epoxy resins using nanoparticles such as nanosilica, nanohalloysite, carbonaceous nanoparticles like graphene nanoplatelets, and graphene oxide [7-13]. However, large scale CFRP production using nanofillers has been a challenge due to many unsolved problems such as nanoparticle agglomeration or achieving homogeneous dispersion of nanoparticles of a high weight/volume portion in resins while maintaining relatively low viscosity. Viscous resin systems cannot easily impregnate continuous fibers or fiber fabrics using fabrication methods based on resin

infusion, and filtering of dense fiber bundles against agglomerated nanofillers can lead to severe segregation and depletion of nanofillers in matrices [14-15].

Alternatively, the use of sizing to improve the poor adhesions between fiber and matrix is a promising approach. Such methods include wet chemical or electrochemical oxidation, plasma treatment, gas phase oxidation, etc. Bubert et al. used oxygen plasma treatment of fibers and changed the surfaces by forming a 1 nm thickness functional group layer to improve the wetting properties of CF [16]. Xu et al. demonstrated that both γ-ray co-irradiation grafting and pro-irradiation grafting were effective methods to improve the interfacial adhesion of composites [17]. But these methods had drawbacks of high energy consumption and could eventually impair the fiber strength.

Polydopamine (PDA) has been reported to have significant applications in numerous biomedical and mechanical areas, due to its superior adhesion to various material surfaces including metals, oxides, polymers, and ceramics [18]. Researchers have reported that PDA could also be applied to modify the surface of nanofillers such as carbon nanotubes [19], graphene [20], and clay [21], revealing its excellent ability to improve the mechanical, thermal, and electromagnetic interference shielding performance of polymer matrices. PDA has also been used to modify the surface of short CFs; the resulting epoxy composites showed distinct improvement in tensile strength and Young's modulus [19]. Recently, much research has been focused on enhancing the interface of CFRP composites, but the effects of PDA sizing modifications of CF surfaces on the crack propagation mechanisms of CFRP have seldom been reported.

In this study, a feasible method of fabricating CFRP by simply using PDA as sizing on carbon fabric has been reported. With 3.2 wt% PDA acting as sizing of CF, the modified CFRP composites can significantly improve energy transfer between CFs and epoxy resin, increasing the friction of fractured interfaces, reducing unstable crack growth, and thereby enhancing interfacial fracture toughness and dynamic impact performance.

2. Experiments

2.1. PDA sizing on carbon fiber fabrics

To prepare PDA coated CF fabrics, first 4 g of dopamine (Sigma, Australia) was dissolved in a mixed solution of deionized water (4000 mL) and aqueous solution of TRIS (3.6 g, 1000 mL) with magnetic stirring for 30 min. Meanwhile, CF fabrics (200 gm plain-weave, Hexcel, USA) were placed in a container. Then, the mixed solution was transferred to the container. The container was shaken by a benchtop orbital shaker (Labec, Australia) at 100 rpm for 24 hrs at ambient temperature. The modified CF fabrics were collected and washed several times with deionized water to remove the residual dopamine, until the scrubbing filtrate became colorless. Finally, the modified CF fabrics were dried in a vacuum oven at 40 ℃ for 24 hrs. Figure 1 shows a schematic drawing of the use of PDA as sizing on the CF surface.

2.2. Preparation of PDA-CFRP composites

A vacuum bagging method was used to fabricate the CFRP composites. First, a release film was placed on a plate and the PDA modified CF fabrics were laid upon it. A release-agent coated release film 10 um in thickness was inserted in the middle layer of the fabrics to induce the initial delamination. After that, a peel cloth and a diversion mesh

were placed on the fabrics and all were sealed in a vacuum bag. Raw resin with the major ingredients of a bisphenol A epoxy (Kinetix R246 epoxy resin, ATL Composites Pty. Ltd., Australia) and a hardener (Kinetix H126, ATL Composites Pty Ltd, Australia) were added at the ratio of 100:25 by weight percent. After layup, epoxy resin was pumped into the vacuum bag. The final panel was cured in a vacuum bag and placed in a hot press machine (Carver Inc. USA) at the pressure of 15 KN/m^2 in room temperature for 24 hrs. The measured cured panel thickness was approximately 3 mm for all plates and the fiber volume was nearly 32 vol.%. Test specimens were cut from the cured panels by bandsaw cutting and polished by a polisher. As controls for evaluation, pure CFRP panels were prepared separately.

2.3. Characterizations

Thermal stability analysis was performed using a thermogravimetric analysis apparatus (Hi-Res TGA 2950, TA instruments, USA). The tests were carried out under N_2 atmosphere at the heating rate of 10.0 ^oC/min from room temperature to 780.0 ^oC. The specimens were vacuum-dried for 2 days at room temperature before TGA characterization. The XPS was performed in an ultrahigh vacuum (UHV) apparatus (SPECS, Germany) with a nonmonochromatic X-ray source for Mg Kα (1253.6 eV) radiation. High-resolution XPS spectra were fitted using combined Gaussian−Lorentzian peaks with background correction using the Shirley method.

The Mode I interlaminar fracture toughness was measured using double cantilever beam (DCB) tests performed by an Instron (U.S.) test machine fitted with a 500 N load cell in accordance with the ASTM D 5528 standard. The dimensions of the DCB specimen were 125×25×3 mm. Specimens were clamped in the jaws of the test machine

via the block hinges, and specimens were loaded at the rate of 1 mm/min while the load–displacement data was recorded. Fracture surfaces of the test specimens were examined and imaged using scanning electron microscopes (Inspect F50, FEI, U.S.). The SEM samples are selected from the pre-crack tip area and all samples were sputter-coated with a ~200 Å layer of gold to minimize charging.

The interlaminar shear strength (ILSS) was measured using a 3-point short beam strength test following the ASTM D-2344 standard. The samples were loaded in a 3-point bending configuration as a simply supported beam using cylindrical supports with the diameter of 3 mm and a loading nose with the diameter of 6 mm. The sample length was 6 times the sample thickness and the span width was set at 4 times the sample thickness. ILSS was calculated from the equation: $\mathrm{ILSS} = 0.75 * \frac{P}{b*d}$, where P represents the breaking load, *b* is the width, and *d* is the thickness of the specimen. At least 8 specimens per batch were tested.

The experiments for the single fiber pull-out test were performed on a Bio Tester 5000 (Cellscale biomaterials testing, Canada) with an optical microscope and two adjustable lights to make *in situ* observations. A constant test speed of 0.05 mm/min was applied.

Impact tests were performed using a 75 J impact hammer on a pendulum impact testing machine (Australian Calibrating Services, Model AC-PIT501J-2, Australia) at room temperature following the ISO-179 standard.

3. Results and discussion

3.1 Effects of polydopamine on carbon fiber

Polydopamine modified CF was prepared using a well-established method based on catecholic chemistry, as shown in Figure 1. The polymerization mechanism of dopamine has been well studied in previous research [19]. The polymerization of PDA on CF surface was examined by SEM (Fig. 2). As shown, the raw CF surface is quite smooth, but the PDA-CF surface is fairly coarse, indicating that the dopamine successfully polymerized on the CF surfaces. Similar morphology was reported by Wang et al. [20].

The surface chemical composition of CF and PDA-CF was investigated by XPS. Figs. 3a and 3b show the survey scan XPS spectra of CF and PDA-CF, respectively. The elemental concentrations demonstrate clearly that carbon and oxygen are the main surface constituents on both CF and PDA-CF surfaces. Nitrogen is found in small concentrations on CF surfaces, possibly deriving from the incomplete carbonization of the PAN-based precursor. Correspondingly, the carbon and nitrogen concentrations are increased on the surfaces of PDA-CF, indicating the sizing of the PDA on the CF surfaces. Figs. 3c-3h are the spectra of C1s, O1s, and N1s on the CF and PDA-CF surfaces, respectively. The high-resolution spectra of PDA are similar with reported XPS results [22]. Compared with CF, it can be seen that the carbon peak at 287.7 eV is contributed from C-N and the peak at 289.4 eV is contributed from C-O-C. As shown in Fig. 3h, the XPS spectrum of the N 1s of PDA-CF is composed of 3 subpeaks centered at 398.5 eV ($–NH_2$), 400.1 eV (–NH–), and 401.8 eV (–N=), respectively. These migrations of N1s binding energy indicate that *in situ* spontaneous oxidative polymerization of dopamine on the CF surface was successfully carried out. Thermogravimetric curves of

CF and PDA-CF are shown in Fig. 4. The weight loss of CF fabric is 8.7 wt% which comes from the original functional groups on the CF surface. In contrast, the PDA-CF fabric loses about 11.9 wt% of the total weight at 800 °C, the 3.2 % weight loses confirming the successful coating of PDA.

3. 2. Mechanical property evaluation in CFRP

To evaluate the effectiveness of this surface modification strategy, Mode I interlaminar fracture toughness was studied in both neat CFRP and PDA-CFRP laminates. Fig. 5(a) shows exemplary load-crack opening displacement (COD) curves obtained from Mode 1 fracture toughness tests at room temperature. The CFRP laminate shows a saw-tooth shaped curve formed as the force alternately increases and decreases, demonstrating unstable energy release during crack propagations. In the PDA-CFRP laminate, however, the force increases regularly to the peak level and then declines in a relatively smooth movement. The COD curves indicate that the PDA-CFRP laminate has the ability to provide an equivalent peak load while eliminating the saw-tooth effect in comparison with the behavior of the pure CFRP laminate. These curves also give evidence that the PDA sizing on the CF is an effective functional method for improving the interfacial load [20]. Fig. 5(b) shows typical Mode I delamination crack growth resistance curves (R-curves) for the CFRP laminates calculated from the load–displacement curves. Generally, the R-curves increase over about the first 10 mm of crack growth, probably as a result of the gradual formation of a fiber bridging zone behind the crack front, that is the main toughening process in these CF composites [23]. The R-curve of the CFRP shows that the interlaminar fracture toughness values (G_{IC}) remain stable in the range of 200-250 J/m^2 beyond the 10 mm of delamination length. Meanwhile, during the DCB test, it was

observed that the delamination propagation progressed at a random rate and in an unstable manner in the neat CFRP laminate. However, the G_{IC} values in the R-curve of the PDA-CFRP laminate are different, with a slight increase in the range of 225-275 J/m^2 beyond 10 mm of delamination length, and during the DCB test the delamination increases at a reasonably consistent speed and in a stable manner. The calculated average value of G_{1c} propagation is 216.34 J/m^2 and 261.25 J/m^2 for the neat CFRP and PDA-CFRP laminates, respectively, showing a 21% increment for the laminate with PDA sizing on fiber surfaces.

The energy translation under the impact test damage mechanisms of the CFRP mainly involve 3 forms: (a) matrix powdering: the brittle epoxy matrix is crushed and forms into debris and powder. Meanwhile, microcrack propagation represents further efforts to convert the impact energy into surface free energy; (b) delamination: the impact energy continues, and delamination occurs around the interface between the CF and epoxy or between the epoxy matrix. Because the delamination transitional zone is very narrow, only small part of the impact energy can be consumed; (c) fiber fracture: at the end of the impact process, when the impact strain is greater than the fiber strain, the CF fails [24]. Fiber/matrix debonding or sliding and fiber pull-out occurs, that consumes a large proportion of the impact energy. The impact strength of the CFRP and PDA-CFRP laminates is 99.89 and 120.12 kJ/m^2 respectively, with about 20% increment with PDA added into the CFRP laminate. The PDA introduced as sizing on the fiber surfaces to enhance the interfacial strength between fiber and epoxy (as shown in the SEM images in Fig. 6) mainly contributes to the energy conversion form of delamination with the

aforementioned damage mechanisms of CFRP, hence increasing the impact strength of the laminate.

The interlaminar shear strength (ILSS) under three-point bending load was found to vary significantly by virtue of the sizing. Composite samples made from PDA-CF had an ILSS of 67.7 Mpa, 25% higher than that of neat CFRP with an ILSS of 54.1 MPa. Table 1 summarizes recent reports of different sizing methods used to improve the ILSS of CFRP. Yuan et al. reported that using the polyacrylate emulsion sizing method increased the ILSS of CFRP by 14.2% [25]. Zhang et al. reported that the use of aqueous epoxy emulsion with different epoxy concentrations of 10%, 15%, and 20%. The best ILSS result came from sizing with 20% epoxy concentration aqueous emulsion with 14.5% increment [26]. Similarly, Kafi et al. reported that electrolytic oxidation and epoxy sizing enhanced the ILSS of CFRP by 17.6% and 70.6% respectively [27]. Zhang et al. reported that with a commercial sizing agent J1 purchased from Japan, the aqueous epoxy emulsion Hit sizing enhanced the ILSS of CFRP from 17.8% to 20.2% [28]. However, the epoxy sizing method, that included three stages of production, namely carbonization, electrolytic oxidation, and epoxy sizing, was environmentally unfriendly compared with our PDA sizing method.

3.3. Enhancement mechanism

To help understand the interface behavior and enhancement mechanism of the PDA-CFRP laminate, the fracture surfaces after the Mode I interlaminar fracture testing were observed by SEM. As evidenced by the clean, smooth surfaces of the fibers shown in Fig. 6(a), the fracture micromechanism in the neat CFRP laminate is primarily interfacial debonding. The epoxy resin completely detaches from the CF surfaces because of the

weak bond in the interfaces. This finding indicates that CF/epoxy debonding is the dominant mechanism of shear failure, and the most likely failure site of the laminates is still the interface. Meanwhile, smooth crazes on the matrix indicate poor resistance to crack propagation. In contrast, in the SEM micrographs as shown in Fig. 6(b), a significantly different interface microstructure appears in the PDA-CFRP fracture surfaces. The fiber/epoxy debonding is combined with resin/resin debonding and fiber pull-out. Significant plastic deformation is shown clearly and an amount of epoxy still adheres to the PDA-CF surface. The development of these microstructures would be related to the enhanced interactions between PDA and epoxy that are responsible for the improvement in interlaminar strength.

Micromechanical tests using single fiber pull-out experiments can simply evaluate interface strength directly [29]. Fig. 7 shows the interfacial stress of CF and PDA-CF from single fiber pull-out testing. The interfacial stress τ was obtained using the equation:

$$\tau = \frac{F}{\pi DL} \quad (1)$$

where F is the measured maximum test load from the test and πDL signifies the fiber-embedded area, which is the product of the fiber-embedded length in epoxy and the circumferential length. The interfacial stress of the CF/epoxy and PDA-CF/epoxy is 12.36 MPa and 15.44 MPa respectively, demonstrating a 25% increment for the PDA/CF epoxy. The PDA enhancement of interfacial strength may results from the PDA attached on the CF surface that increases the friction of the fractured interface. Schematic diagrams and micro-morphologies of interface debonding in the neat CFRP are displayed in Fig. 8(a), where the epoxy resin tends to wholly detach from the CF and retain a comparatively clean surface. This response is due to the weak binding energy between

the epoxy and CF surfaces. In the DPA-CFRP on the other hand, the crack propagates through the interfaces of PDA /epoxy with non-straight crack paths and the leftover fiber is captured by the abundant epoxy, as shown in Fig. 8(b). This response indicates that the PDA sizing enhances the interface layer by improving the load transfer between epoxy and CF surfaces.

4. Conclusions

In this study, 3.2 wt% polydopamine was used as sizing on CF fabrics. The results showed that the modified CF fabrics significantly enhanced the mechanical properties of the CFRP laminates, with a 20-25% increment obtained for Mode I interlaminar fracture toughness, impact strength, interlaminar shear strength, and interfacial stress compared with pure CFRP. More importantly, the crack propagation behavior during the Mode I interlaminar fracture toughness evaluation changed from saw-tooth-shaped curves for neat CFRP to relatively smooth curves. The enhanced mechanism was mainly due to significantly increased interfacial bonding between epoxy resin and CF by the PDA sizing. The PDA layer also improved the load transfer between CFs and polymer matrix, increasing the fractured interface friction and reducing unstable crack growth, and thereby enhancing interfacial fracture toughness and impact performance.

Acknowledgement

W Han is grateful for the research training program scholarship during his PhD study.

References

[1] Maugis D. Subcritical crack growth, surface energy, fracture toughness, stick-slip and embrittlement. J Mater Sci 1985; 20 (9): 3041-3073.

[2] Ghasemnejad H, Hadavinia H, Aboutorabi A. Effect of delamination failure in crashworthiness analysis of hybrid composite box structures. Mater Des 2010; 31 (3): 1105-1116.

[3] Maksimov IL. Thermomechanical fracture instability and stick-slip crack propagation. Appl Phys Lett 1989; 55 (1): 42-44.

[4] Kinloch AJ, Williams JG. Crack blunting mechanisms in polymers. J Mater Sci 1980; 15: 987-996.

[5] Lee C, Wei X, Kysar JW, Hone J. Measurement of the elastic properties and intrinsic strength of monolayer graphene. Science 2008; 321 (5887): 385-388.

[6] Qin W, Vautard F, Drzal LT, Yu J. Mechanical and electrical properties of carbon fiber composites with incorporation of graphene nanoplatelets at the fiber-matrix interphase. Compos Part B 2015; 69: 335-341.

[5] Hamer S, Leibovich H, Green A, Avrahami R, Zussman E, et al. Mode I and mode II fracture energy of MWCNT reinforced nanofibril mats interleaved carbon/epoxy laminates. Compos Sci Techno. 2014; 90: 48-56.

[6] Lee SH, Kim H, Hang S, Cheong SK. Interlaminar fracture toughness of composite laminates with CNT-enhanced nonwoven carbon tissue interleave. Compos Sci Technol 2012; 73 (1): 1-8.

[7] Wicks SS, Villoria RG, Wardle BL, Interlaminar and intralaminar reinforcement of composite laminates with aligned carbon nanotubes. Compos Sci Technol 2010; 70 (1): 20-28.

[8] Chi Y, Chu J, Chen M, Li C, Mao W, et al. Directly deposited graphene nanowalls on carbon fiber for improving the interface strength in composites. Appl Phys Lett 2016; 108 (21): 211601.

[9] Ning H, Li J, Hu N, Yan C, Liu Y, et al. Interlaminar mechanical properties of carbon fiber reinforced plastic laminates modified with graphene oxide interleaf. Carbon 2015; 91: 224-233.

[10] Irshidat MR, Al-Saleh MH, Almashagbeh H. Effect of carbon nanotubes on strengthening of RC beams retrofitted with carbon fiber/epoxy composites. Mater Des 2016; 89: 225-234.

[11] Zhang RL, Gao B, Du WT, Zhang J, Cui HZ, et al. Enhanced mechanical properties of multiscale carbon fiber/epoxy composites by fiber surface treatment with graphene oxide/polyhedral oligomeric silsesquioxane. Compos A: Appl Sci Manuf 2016;84: 455-463.

[12] Zhang P, Ma L, Fan F, Zeng Z, Peng C, et al. Fracture toughness of graphene. Nat Commun 2014; 5: 3782, doi: 10.1038/ncomms4782.

[13] Zhang X, Fan X, Yan C, Li H, Zhu Y, Li X, Yu L. Interfacial microstructure and properties of carbon fiber composites modified with graphene oxide. ACS Appl Mater Interfaces 2012; 4 (3): 1543-1552.

[14] Yu B, Jiang Z, Tang XZ, Yue CY, Yang J. Enhanced interphase between epoxy matrix and carbon fiber with carbon nanotube-modified silane coating. Compos Sci Technol 2014; 9: 131-140.

[15] Han W, Tang YH, Ye L. Chapter 8: Carbon Fiber-Reinforced Polymer Laminates with Nanofiller-Enhanced Multifunctionality. In: Beaumont PWR et al, editors. The Structural Integrity of Carbon Fiber Composites. Switzerland: Springer, 2017, p 171-189.

[16] Bubert H, Ai X, Haiber S, Heintze M, Brüser V, Pasch E, et al. Basic analytical investigation of plasma-chemically modified carbon fibres. Spectrochim Acta B 2002; 57: 1601-1610.

[17] Xu ZW, Huang YD, Zhang CH, Liu L, Zhang YH, Wang L. Effect of c-ray irradiation grafting on the carbon fibres and interfacial adhesion of epoxy composites. Compos Sci Technol 2007; 67: 3261-3270.

[18] Lynge ME, Westen R, Postma A, Stadler B. Polydopamine- a nature-inspired polymer coating for biomedical science. Nanoscale 2011; 3(12): 4916-4928.

[19] Liu X, Wang G, Liang R, Shi L, Qiu J. Environment-friendly facile synthesis of Pt nanoparticles supported on polydopamine modified carbon materials. J Mater Chem A 2013; 1: 3945-3953.

[20] Wang PF, Yang JL, Liu WS, Tang XZ, Zhao K, Lu XH, et al. Tunable crack propagation behavior in carbon fiber reinforced plastic laminates with polydopamine and graphene oxide treated fibers. Mater Des 2017; 113: 68-75.

[21] Liaqat F, Tahir MN, Huesmann H, Daniel P, Kappl M, et al. Ultrastrong composites from dopamine modified-polymer-infiltrated colloidal crystals. Mater Horiz 2015; 2: 434-441.

[22] Qu KG, Zheng Y, Jiao, Y, Zhang XX, Dai S, Qiao SZ. Polydopamine-inspired, dual heteroatom-doped carbon nanotubes for highly efficient overall water splitting. Adv Energy Mater 2017; 1602068.

[23] Mouritz AP, Baini C, Herszberg I. Mode I interlaminar fracture toughness properties of advanced textile fiberglass composites. Compos part A 1999; 30: 859-870.

[24] Yang Y, Xu F, Zhang YQ, Liu GW. Experimental study on the impact resistance of 2D plain-woven C/SiC composite. Ceram Int 2014; 10(40): 15551-15559.

[25] Yuan X, Zhu B, Cai X, Liu J, Qiao K, Yu J. Optimization of interfacial properties of carbon fiber/epoxy composites via a modified polyacrylate emulsion sizing. Appl Surf Sci 2017; 401: 414-423.

[26] Zhang R, Huang Y, Liu L, Tang Y, Su D, Xu L. Influence of sizing emulsifier content on the properties of carbon fibers and its composites. Mater Des 2012; 33: 367-371.

[27]. Kafi A, Huson M, Creighton C, Khoo J, Mazzola L, et al. Effect of surface functionality of PAN-based carbon fibres on the mechanical performance of carbon/epoxy composites. Compos Sci Technol 2014; 94: 89-95.

[28] Zhang RL, Zhang JS, Zhao LH, Sun YL. Sizing agent on the carbon fibers surface and interface properties of its composites. Fiber Polym 2015; 16: 657-663.

[29] Sethi S, Ray BC. Environmental effects on fibre reinforced polymeric composites: Evolving reasons and remarks on interfacial strength and stability. Adv Colloid Interface Sci 2015; 217: 43-67.

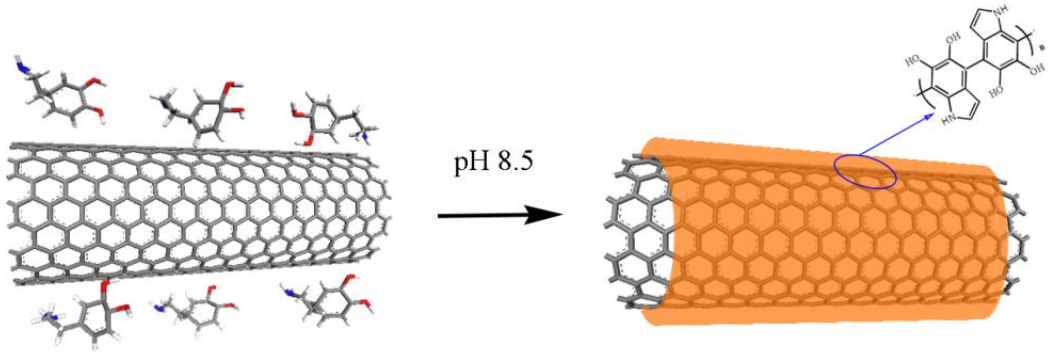

Fig. 1. Schematic diagram of polydopamine coating on a CF surface and acting as sizing.

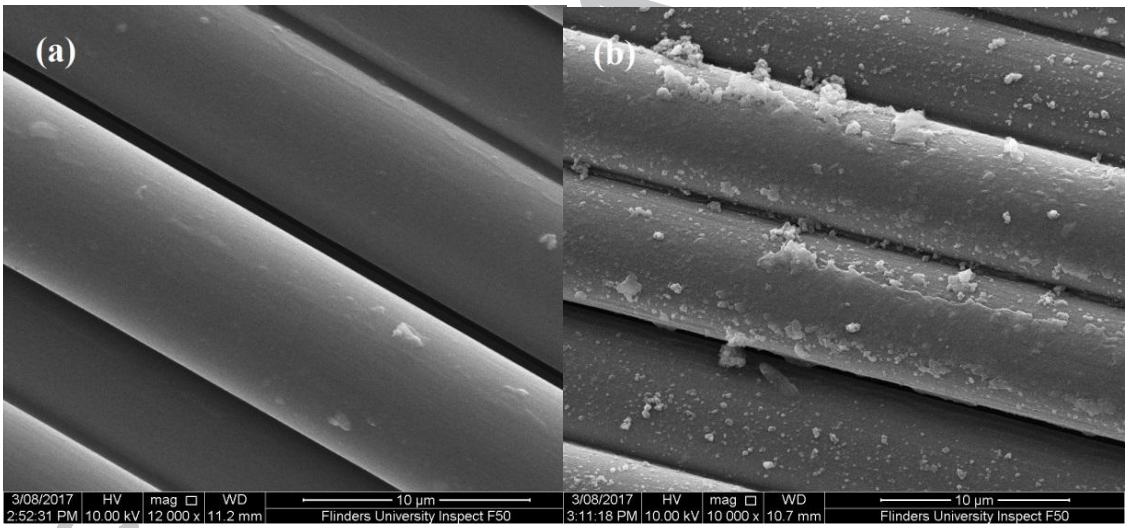

Fig. 2. SEM images of (a) CF and (b) PDA -CF surfaces.

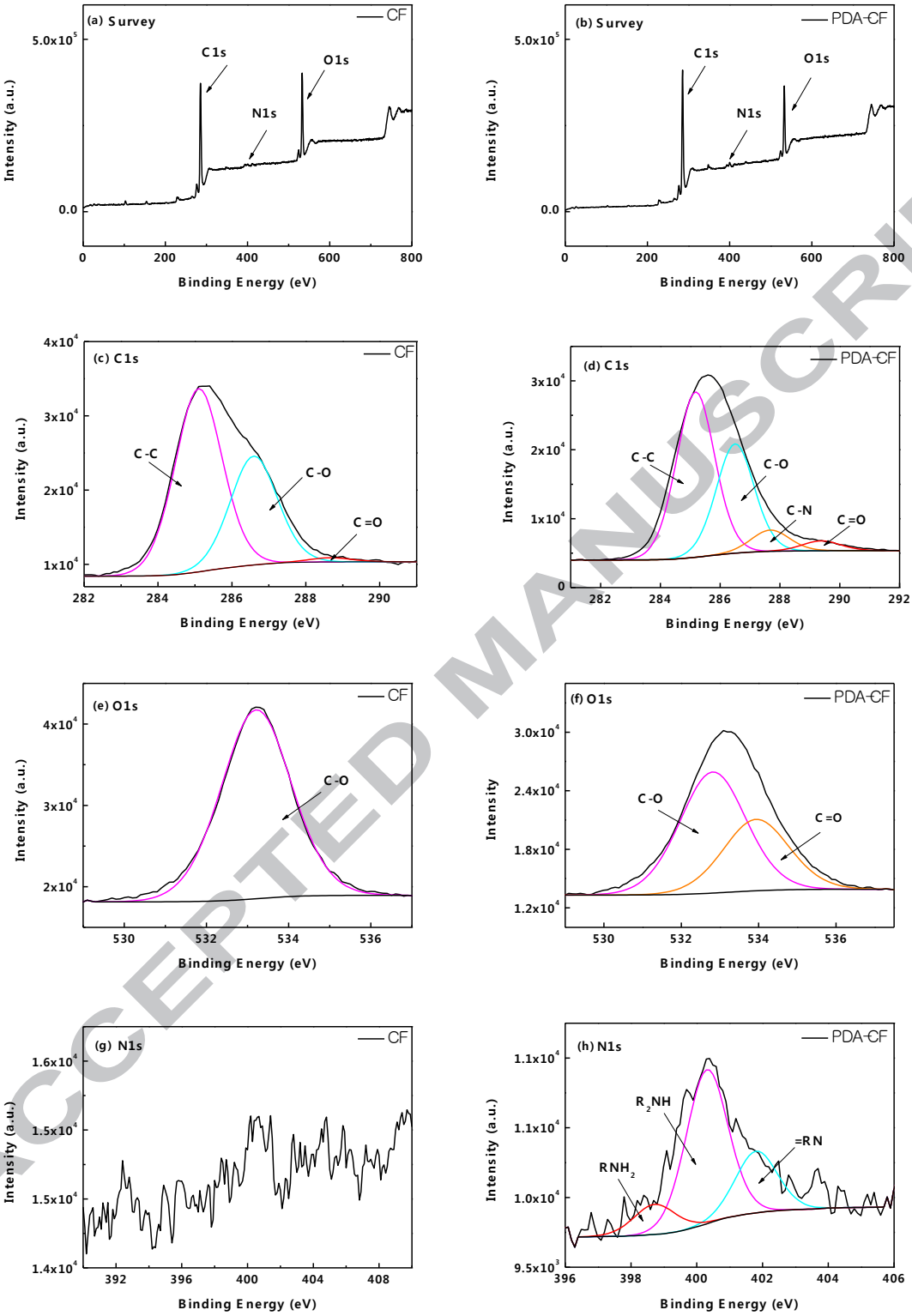

Fig. 3. The XPS spectra of CF and PDA-CF.

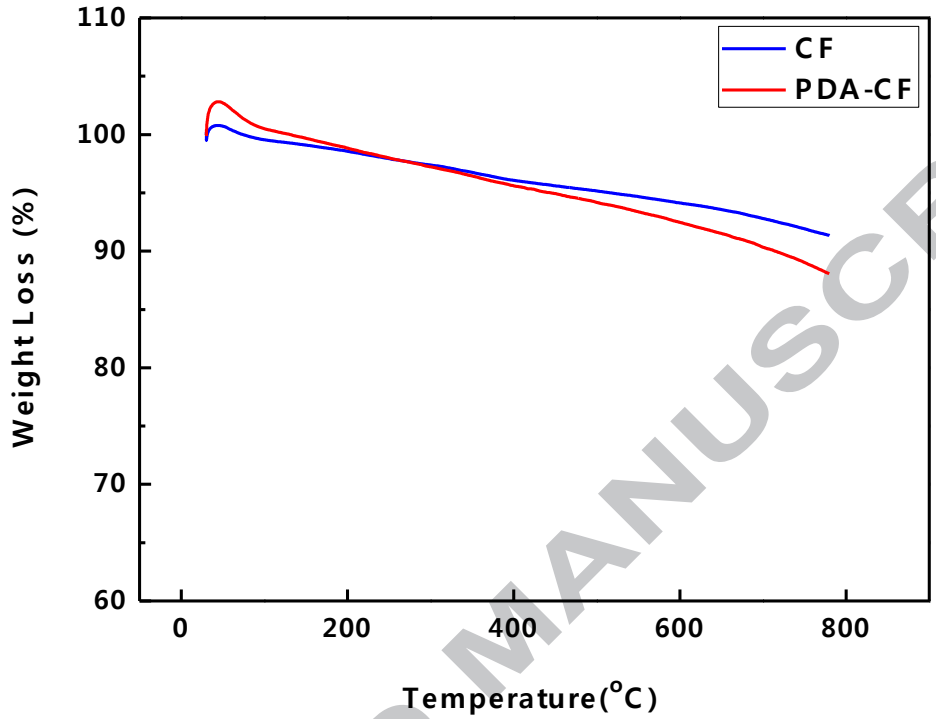

Fig. 4. Thermogravimetric analysis shows the PDA concentration on the CF surfaces.

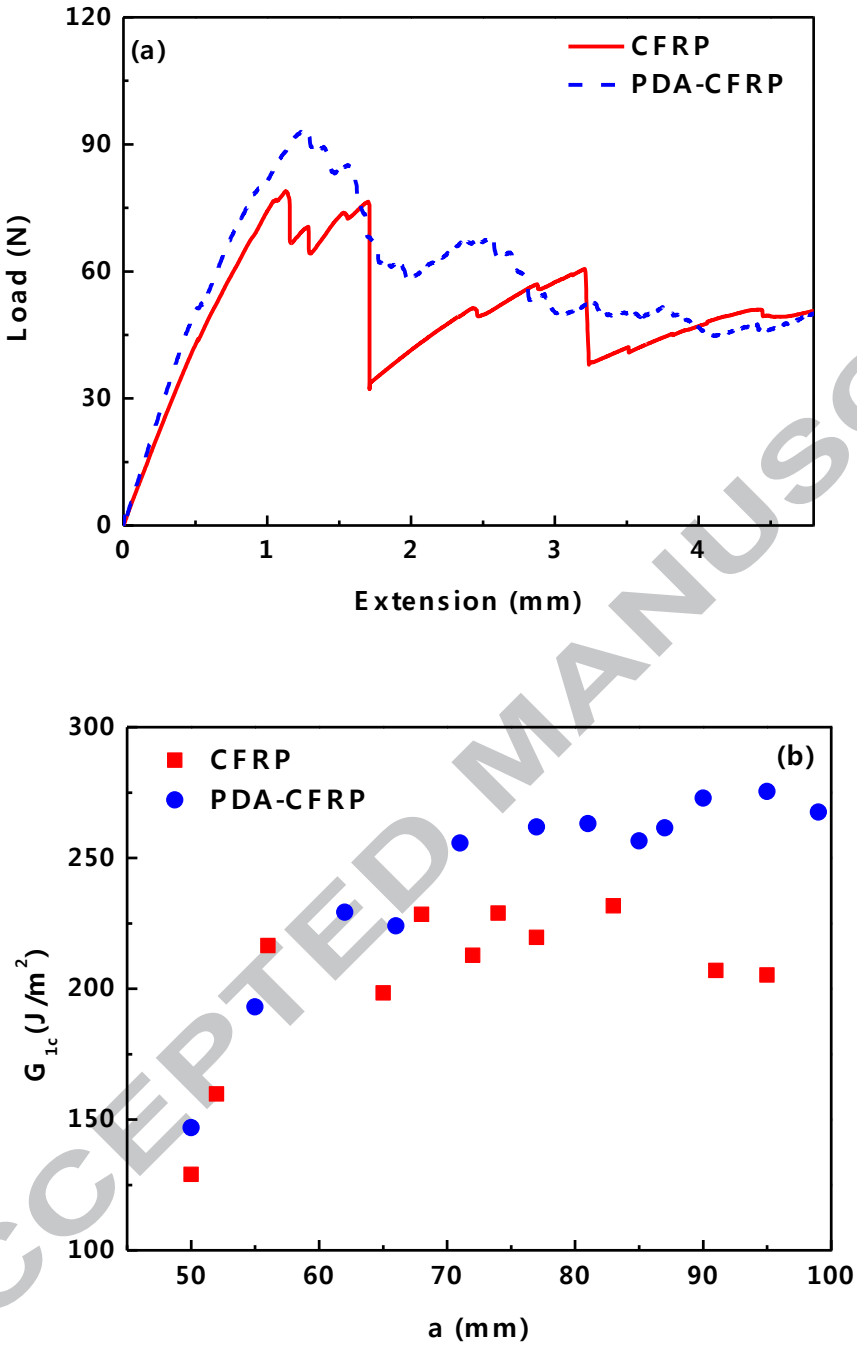

Fig. 5. (a) Load-crack opening displacement (COD) curves and (b) mode I delamination crack growth resistance curves (R-curves) of CFRP and PDA-CFRP laminates.

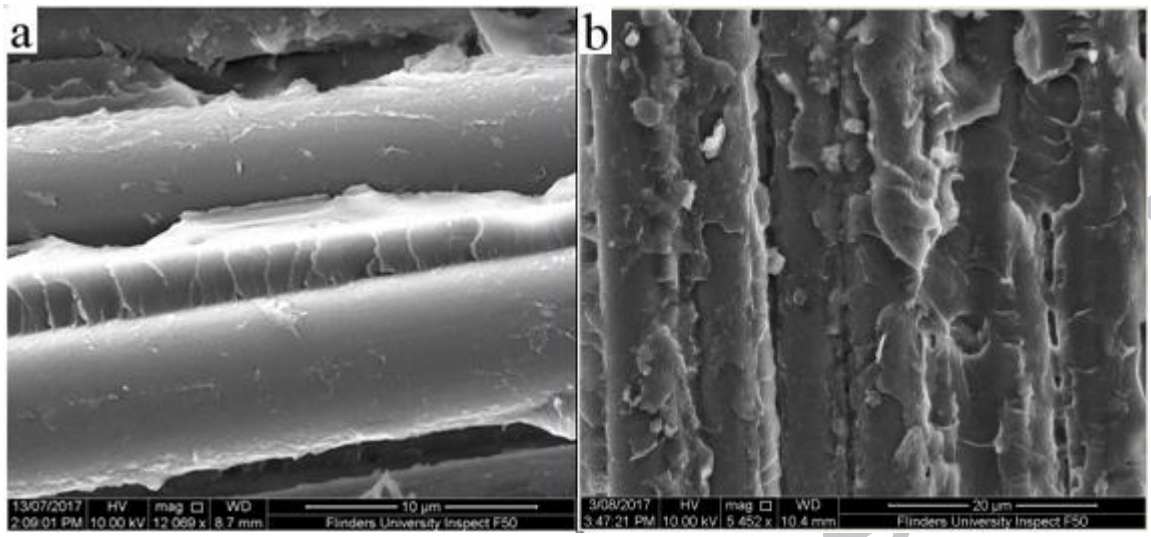

Fig. 6. SEM images of the fracture surfaces after Mode I interlaminar fracture testing of (a) CFRP and (b) PDA-CFRP.

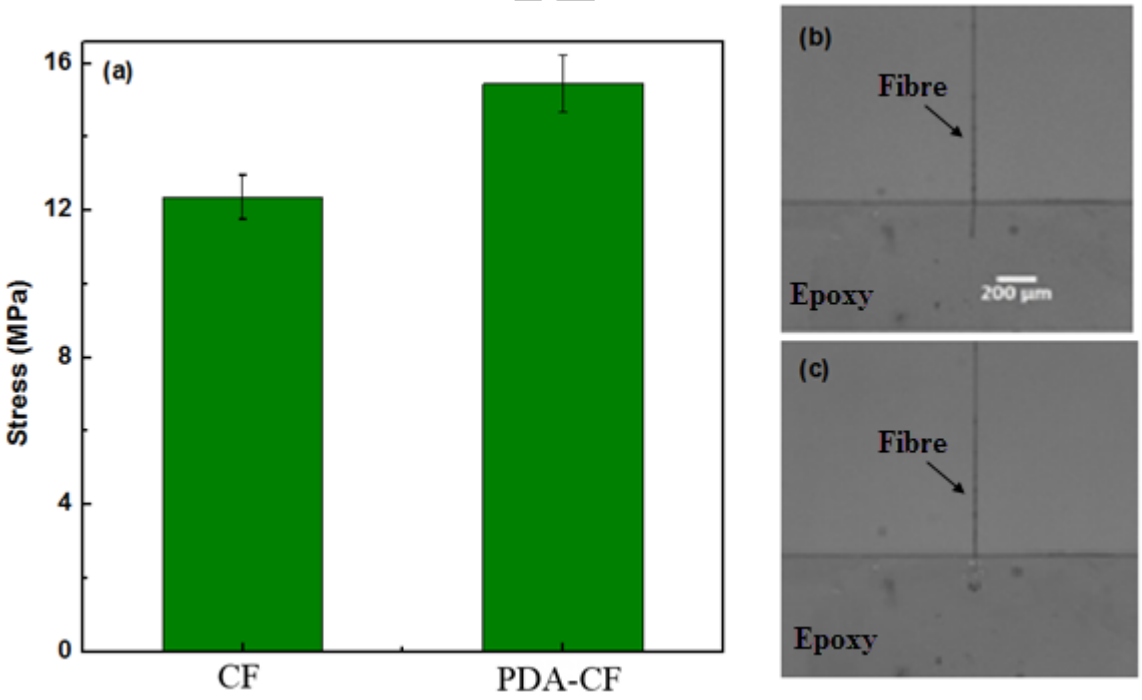

Fig. 7. (a) Interfacial stress for CF and PDA-CF by single fiber pull-out testing, and images of a single fiber (b) before and (c) after pull-out.

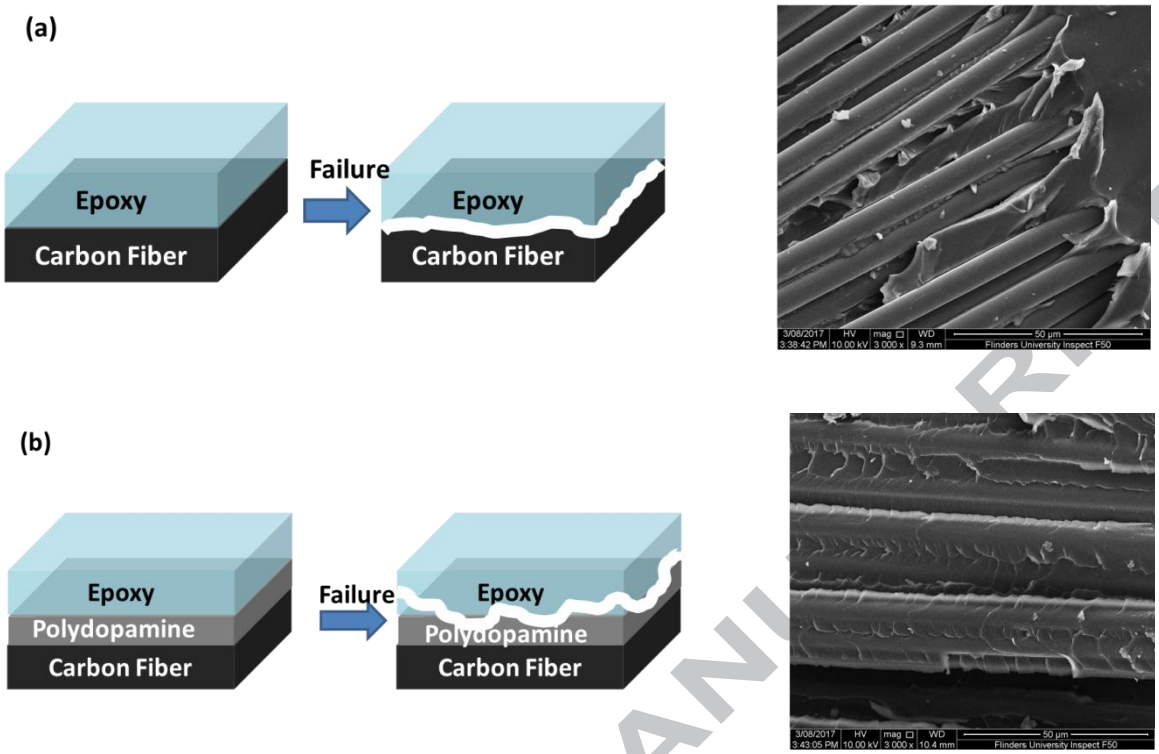

Fig. 8. Schematic diagrams and micro-morphologies of interface failure in (a) CFRP and (b) PDA-CFRP laminates.

Table 1: Improvement of ILSS by different sizing methods.

Sizing material		Epoxy	ILSS (MPa)	Improvement (%)	Ref.
PDA		Kinetix R246	67.7	25.1	Current study
Polyacrylate emulsion		Epoxy 616	92.7	14.2	25
Aqueous epoxy resin emulsion	E-1	Epoxy 616	82	1	26
	E-2		88	8.4	
	E-3		93	14.5	
J1 sizing		Epoxy 616	84	17.8	27
Hit sizing			85.7	20.2	
Oxidized Epoxy sizing		Epikote Rimr 935	40	17.6	28
			58	70.6	